Vortex liquid entanglement in twinned $YBa_2Cu_3O_7/Y_2BaCuO_5$ composite superconductors

T. Puig and F. Galante
Institut de Ciència de Materials de Barcelona–CSIC, Campus UAB, 08193 Bellaterra, Spain

E. M. González and J. L. Vicent
Departamento de Física de Materiales, Facultad de Física, Universidad Complutense, 28040 Madrid, Spain

B. Martínez and X. Obradors
Institut de Ciència de Materials de Barcelona–CSIC, Campus UAB, 08193 Bellaterra, Spain

(Received 2 June 1999)

The angular dependence of the in-plane resistivity $\rho(T,H,\theta)$ of melt textured $YBa_2Cu_3O_7/Y_2BaCuO_5$ composites has been measured in a large range of magnetic fields and temperatures and from them, the intrinsic anisotropy of the superconducting state has been verified following the anisotropic Ginzburg-Landau approach. The influence of correlated defects like twin boundaries and quenched disorder generated by Y_2BaCuO_5 precipitates on the pinning behavior of these composites in the liquid vortex state is analyzed, and the corresponding phase diagram is determined and compared to that of twinned single crystals. We show that the irreversibility line displays an upwards shift due to twin boundary pinning enabling to define a ''quenched'' Bose glass transition. A new region in the vortex liquid state is identified where twin boundary pinning defines a partially entangled liquid vortex state characterized by a short-range *c*-axis vortex coherence. The transition to the entangled liquid phase is experimentally determined. The relevance of this depinning line and its unique position with respect to twinned single crystals is discussed. [S0163-1829(99)01741-5]

I. INTRODUCTION

The study of vortex line dynamics and its relationship with different kinds of defects is one of the major topics in the search for understanding the vortex matter of high-temperature superconductors.

In clean $YBa_2Cu_3O_7$ superconductors, a first-order vortex lattice melting transition has been clearly identified either through dynamic[1,2] or equilibrium physical measurements.[3,4] This thermodynamic state of the flux-line lattice is easily destroyed, however, with the introduction of pointlike random disorder such as that generated by proton irradiation[5,6] or by the introduction of linearly correlated defects such as columnar tracks induced via heavy-ion irradiation[7–9] and naturally growing twin boundaries.[10,11] In the first case, an entanglement of vortex lines is promoted in the liquid state by vortex pinning in these defects. Then the transition to the solid state occurs as a second-order vortex glass transition.[12] In the second case, a new solid vortex state is achieved through a second-order phase transition that was defined by Nelson and Vinokur[13] as a Bose glass transition. This new solid phase is characterized by pinning of vortices in linearly correlated defects, thus promoting vortex localization and inhibiting vortex wandering. The vortex rigidity increases up to displaying an infinite tilt modulus C_{44} at the phase transition and hence, a strong enhancement of vortex pinning is attained.

Remarkably, the influence on vortex pinning by linearly correlated twin boundaries becomes still visible in the vortex liquid state. Experimentally, the clearest methodology to visualize the influence of twin boundaries is to study the anisotropy dependence of the transport and magnetic properties. In single crystalline $YBa_2Cu_3O_7$, the anisotropic magnetoresistance was shown to present a dip when the magnetic field crosses the twin boundaries either within the *ab* plane[14] or rotating from the *c* axis to the *ab* plane.[10] Also the irreversibility line was shown to display an upward shift for $H\|c$ due to twin boundary pinning, superposed to an anisotropic background. It was demonstrated[9,15] that the *c*-axis coherence of vortices in the liquid state was consequently strongly enhanced. All these investigations resulted in the identification of a disentangled vortex liquid phase in a small H-T region above the Bose glass transition, induced by linearly correlated defects.[16,17]

Melt textured bulk $YBa_2Cu_3O_7$ is an interesting class of superconducting ceramic material because several structural defects coexist and hence, may display competing pinning effects leading to new complex behaviors. The main microstructural defect of this material is the micrometric Y_2BaCuO_5 (211) precipitates, which are randomly distributed within the superconducting matrix and which strongly enhance vortex pinning in the solid state.[18,19] In the liquid state, however, the random distribution of 211 particles within the matrix should promote vortex entanglement. Thus, the study of the transport properties, which reflects the dynamic behavior of the vortex lattice, should enable the determination of the interplay between the quenched random disorder added by 211 particles and the correlated disorder induced by twin boundaries. As a result of this competing effect between both microstructural defects, it was recently suggested, based on transport measurements with the flux transformer geometry,[20] that a partially disentangled state could exist in a narrow region of the liquid vortex phase diagram of melt-textured materials. This new vortex state would consist of short segments of vortex lines with a finite coherence along the *c* axis.

In this work, we further investigate the vortex liquid state of melt-textured $YBa_2Cu_3O_7/Y_2BaCuO_5$ (Y123/211) superconducting composites by means of anisotropic magnetoresistance measurements. From these measurements, we give first compelling evidence for an intrinsiclike anisotropy calculated where thermal activation has completely washed out any defect pinning effect in the vortex liquid state, and we confirm the high-crystalline orientation of this composite material.

At lower temperatures, we identify the new liquid vortex state having short-range vortex correlation. In this phase, vortex pinning by twin boundaries enhances the liquid viscosity, while random 211 particles induce plastic shear of the flux-line lattice and flux cutting. This region of the phase diagram H-T-θ determined by the partially disentangled liquid vortex state is identified and we show that in this new state the ''quenched'' disorder induced by the 211 particles is relevant to perturb, though not overwhelm, the effect of the linearly correlated twin boundary disorder. Finally, we show that a ''quenched'' Bose glasslike transition line remains well defined. The latter will be compared to the irreversibility line that should be observed in the absence of any correlated disorder and also to the true Bose glass line of a twinned single crystal. Overall, a complete magnetic phase diagram of the vortex liquid state is outlined for melt-textured Y123/211 superconducting composites and it is compared to that observed in twinned $YBa_2Cu_3O_7$ single crystals. Our work stresses the positive influence of twin boundaries as an effective source of flux pinning in the liquid state and their success in retaining the entrance to the entangled state until a depinning line $H_{TB}(T)$ is surpassed against the competing effect of the quenched disorder induced by the 211 particles. A strong resemblance of this new $H_{TB}(T)$ line in the phase diagram, separating the entangled and disentangled liquid state, is found with that predicted theoretically by Nguyen and Sudbo[21] as an intrinsic second-order phase transition of type-II superconductors. This line was predicted to be characterized by a loss of vortex line tension and its position should not depend on the particular characteristic of the line defect allowing to visualize it. A comparison between single crystals and melt-textured composites is performed in this latter framework.

II. EXPERIMENT

Single domain $YBa_2Cu_3O_{7-d}/Y_2BaCuO_5$ (Y123/211) melt-textured composites were grown by a modified Bridgman directional solidification technique in air and oxygenated at 450 °C in 1 bar of O_2 during 120 h. Details of sample preparation have been reported elsewhere.[22] Similar results were obtained for several samples of different 211 content. The results here reported belong to samples with a 28 wt % of 211 whose critical current density at 77 K in self-field was $J_c^{ab}=7\times10^4$ A/cm^2.[19] The actual content of 211 phase retained into the single domain was determined by measuring the high-temperature Curie-Weiss paramagnetic susceptibility arising from the 211 phase.[19] Upon oxygenation of the samples, polarized light optical microscopy analysis revealed a random distribution of 211 particles with mean sizes of 1 μm and a high density of twin boundaries showing the two orthogonal families. Typical separation between twin boundaries in these melt-textured composites is ~100 nm. The superconducting transition temperature, defined as the midpoint transition, was found at 91.3 K with $\Delta T_c\sim0.5$ K (Fig. 1). Small pieces of about $1.5\times1\times0.2$ mm^3 were cleaved from the *ab* plane and their in-plane magnetoresistance was measured by using the standard four-point technique. Contact resistances better than 0.1 Ω were obtained by properly masking the samples before a gold sputtering deposition. Four Pt wires were then attached to the gold contacts using silver epoxy and finally, the contacts were cured at 300 °C in flowing oxygen. The magnetoresistance measurements were performed in a He^4 cryostat provided with a 9-T superconducting magnet and a rotometer that enabled rotation of the magnetic field from the crystallographic *c* axis of the sample ($\theta=0°$) to the *ab* plane ($\theta=90°$) with a resolution of 0.1°. Measurements were performed with an *ac*-transport current of 100 μA applied along the *ab* plane and ensuring orthogonality with the magnetic field when the latter was aligned within the *ab* plane.

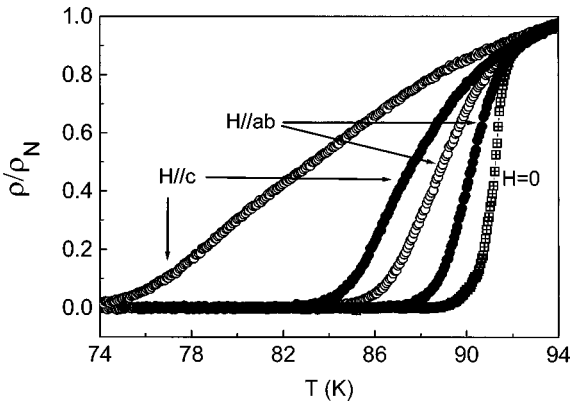

FIG. 1. Temperature dependence of the magnetoresistance for $H\|c$ ($\theta=0°$) and $H\|ab$ ($\theta=90°$) and magnetic fields of (●) 3 T and (⊙) 9 T. Also shown (⊞) is the resistive transition for $H=0$ T.

III. RESULTS AND DISCUSSIONS

A. Intrinsic anisotropy

Figure 1 shows the temperature dependence of the in-plane magnetoresistance for $H\|c$ ($\theta=0°$) and $H\|ab$ ($\theta=90°$) and magnetic fields of 3 and 9 T, as representative data. The resistive transition broadens as the magnetic field increases, both for $H\|c$ and $H\|ab$, reaching ΔT_c values of up to 16 K for $H\|c$ at 9 T. Note that the resistive transition drops smoothly to zero as a sign of a second-order phase transition from the liquid vortex state to the solid vortex state, which is representative of a glassy system dominated by microstructural defects.[23] No resistance kink associated to the first-order melting transition, observed in clean crystals,[2] appears in our measurements. It is also shown that the resistivity for $\theta=0°$ and $\theta=90°$ differs and that the in-plane resistivity might be equal to zero for $H\|ab$ while it still stays discrete for $H\|c$. This evidences the intrinsic anisotropy of this layered material.

In order to determine the intrinsic anisotropy of these melt-textured composites so longer discussed, and compare it with that of Y123 single crystals, we present in Fig. 2 the

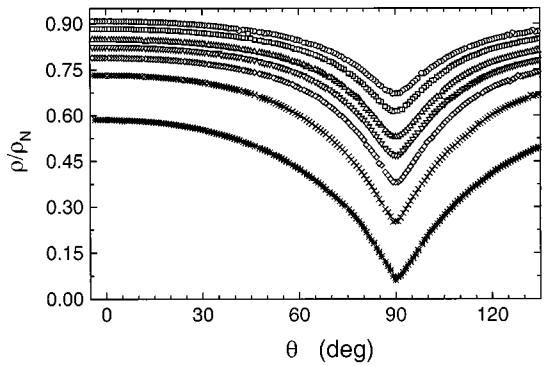

FIG. 2. Angular-dependent magnetoresistance at $t=T/T_c=0.995$ for the magnetic fields (upper curve to bottom curve) of 1, 2, 3, 4, 5, 7, and 9 T.

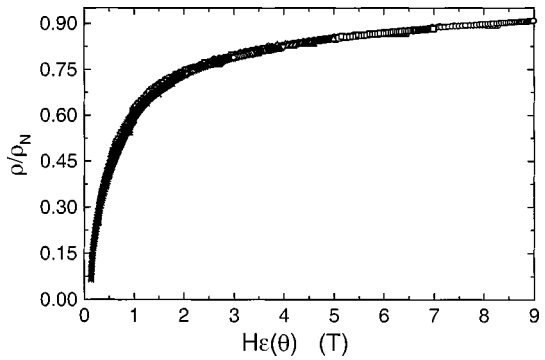

FIG. 3. Anisotropic Ginzburg-Landau model scaling for resistivity data of Fig. 2. Notice the universal scaling law obtained.

angular-dependent magnetoresistance at $T/T_c\sim 0.995$ for $H=1$, 2, 3, 4, 5, 7, and 9 T. We have analyzed these results on the basis of the anisotropic Ginzburg-Landau model,[24] which assumes an anisotropy of the upper critical field given by the expression:

$$\left[\frac{H_{c2}(\theta)\sin\theta}{H_{c2}^{ab}}\right]^2+\left[\frac{H_{c2}(\theta)\cos\theta}{H_{c2}^{c}}\right]^2=1, \qquad (1)$$

where H_{c2}^{ab} and H_{c2}^{c} are the upper critical fields parallel to the *ab* plane and to the *c* axis, respectively. Since the experimental determination of H_{c2} is not obvious for high-temperature superconductors[25] due to the relevance of fluctuation effects, we have used the scaling approach suggested by Blatter *et al.*[26] for the study of anisotropic superconductors. The essential assumption is that, within the Ginzburg-Landau approach, physical measurements of anisotropic superconductors may be generalized from those of isotropic superconductors if a reduced magnetic field $H_{\rm red}$ is defined,

$$H_{\rm red}=H\varepsilon(\theta)=H(\cos^2\theta+\gamma^2\sin^2\theta)^{1/2}, \qquad (2)$$

where $\varepsilon(\theta)$ is the anisotropy factor and $\gamma=H_{c2}^{c}/H_{c2}^{ab}=(m_{ab}/m_c)^{1/2}$ is the inverse of the anisotropy parameter related to the ratio of the effective masses and which has been found to be in the range $6<\gamma^{-1}<8$ for the Y123 system.[27–29] Previously, similar analysis performed in $EuBa_2Cu_3O_7/PrBa_2Cu_3O_7$ superconducting multilattices[30] had enabled us to investigate the anisotropy of artificial structures.

Figure 3 demonstrate the validity of the scaling-law approach for the curves of Fig. 2 of the melt-textured composite. Note that a very good scaling agreement is observed for all magnetic fields and angles, which evidences that the anisotropic Ginzburg-Landau model is suitable to explain the intrinsic anisotropy of the superconducting state of melt-textured Y123/211 composites. These measurements were performed at high temperatures $t=T/T_c=0.995$ to ensure that thermal activation is high enough to neglect any residue of vortex pinning and to ensure a three-dimensional (3D) line behavior of the vortices.[36] The value for the anisotropy parameter determined from this scaling is $\gamma^{-1}\sim 7$, which indicates that melt-textured Y123 composites have a very high-crystalline quality and that this is not modified by the presence of the Y211 particles. A similar scaling approach was successfully used by Kwok *et al.*[31] to describe the anisotropy of the vortex lattice melting temperature at constant field $T_m(\theta)$ in untwinned $YBa_2Cu_3O_7$ single crystals.

Therefore, we confirm that the scaling of the magnetoresistance is very efficient to determine the intrinsic anisotropy of high-temperature superconductors and that melt-textured composites do have the same anisotropy parameter as single crystals, even if x-ray-diffraction (XRD) rocking curves display mosaicities in the range of $\Delta\theta\sim 3°-5°$.[32] These results give a definitive support to the consideration of Y123/211 composites as a quasi-single-crystalline material. On the other hand, it warns us on the fact that care should be taken when determining the anisotropy parameter from methods that might be influenced by flux-pinning effects such as ratios of critical current densities J_c^{ab}/J_c^{c}, and irreversibility fields $H_{\rm irr}^{ab}/H_{\rm irr}^{c}$.[33,34] Initially contradictory results might give coherent values if re-examined by subtracting the influence of flux-pinning effects. Specially, in the case of melt-textured composites since they have a very rich microstructure, i.e., 211 particles, twin boundaries, dislocations, stacking faults, etc.[32] which, depending on the magnetic field direction, affect in different degrees the properties of the material. Hence, a misleading anisotropy of the material might be inferred.[35] An analysis of the anisotropy of melt-textured composites in the pinned liquid vortex state is performed in the next section. There, we have used angular-dependent magnetoresistance measurements to separate the contributions of the different flux-pinning effects from that of the intrinsic anisotropy.

B. Anisotropy in the pinned vortex liquid state

Figure 4 shows the angular-dependent magnetoresistance for the Y123/211 melt-textured composite at lower temperatures, $t=T/T_c=0.964$ and $t=T/T_c=0.832$, for a magnetic field of 1 and 9 T, respectively. The transport current was applied parallel to one of the twin boundary families, thus when the magnetic field was applied along the *c* axis, the Lorentz force was exerted perpendicular to that twin boundary family. The overall anisotropic character of the material is visible in Fig. 4. However, at $\theta\sim 0$ ($H\|c$) a dip appears in the magnetoresistance, indicating a non-negligible decrease of dissipation around this particular magnetic field orientation and which should be ascribed to pinning by anisotropic defects mainly active for $H\|c$.

Y123/211 melt-textured composites have a very rich microstructure, as already mentioned, with different types of

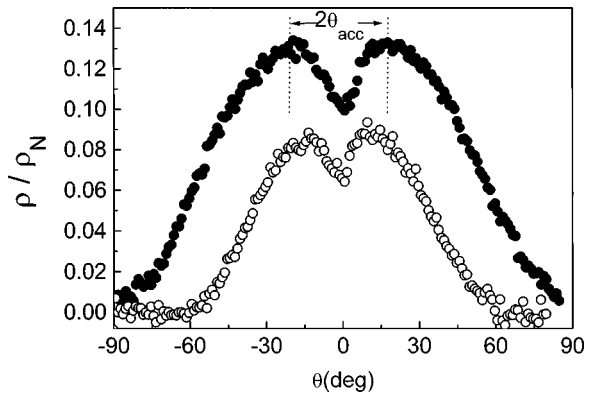

FIG. 4. Angular-dependent magnetoresistance at (●) $t=T/T_c=0.964$ at 1 T and (❍) $t=0.832$ at 9 T, where a decrease of dissipation is obtained for $\theta\sim 0°$.

defects.[32] However, they do possess two dominant defect contributions to flux pinning: (i) 211 precipitates that are mainly spherical and thus isotropic in relation to the magnetic field orientation, especially in the liquid vortex state where vortex wandering is promoted,[36] and (ii) a dense twin boundary structure along the {110} planes that should act as anisotropically linear correlated pinning centers for $H\|c$. Therefore, the decrease of dissipation observed in Fig. 4 for $\theta\sim 0$ has been ascribed to twin boundary pinning. From these measurements we can identify an accommodation angle $\theta_{\rm acc}$ that defines the maximum deviation from {110} directions of the vortex lines to still remain partially trapped to the twin boundaries. The $\theta_{\rm acc}$ values observed in Fig. 4 are $|\theta_{\rm acc}|\sim 20°$ for $H=1$ T at $t=0.964$ and $|\theta_{\rm acc}|\sim 12°$ at 9 T and $t=0.832$. These angles are comparable with those observed in twinned single crystals[10] and splayed defects[37] and somewhat smaller than that of columnar tracks induced by U irradiation.[9] Further analysis on the accommodation angle $\theta_{\rm acc}$, its temperature and magnetic field dependence and its relation to the twin boundary pinning energy will be reported elsewhere.[38]

The scaling of magnetoresistivity following Eq. (2) for $t=T/T_c=0.931$ and 1, 3, 6, and 9 T is shown in Fig. 5. Data

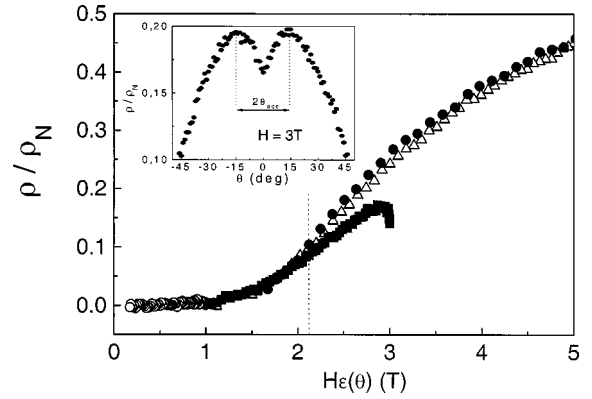

FIG. 5. Scaling of the anisotropic Ginzburg-Landau model of the angular-dependent magnetoresistance at $t=T/T_c=0.931$ and 1, 3, 6, and 9 T. Also shown in the inset is the angular-dependent magnetoresistance curve for $H=3$ T at $t=0.931$, in the region where a clear divergence from the mean-field scaling law is observed.

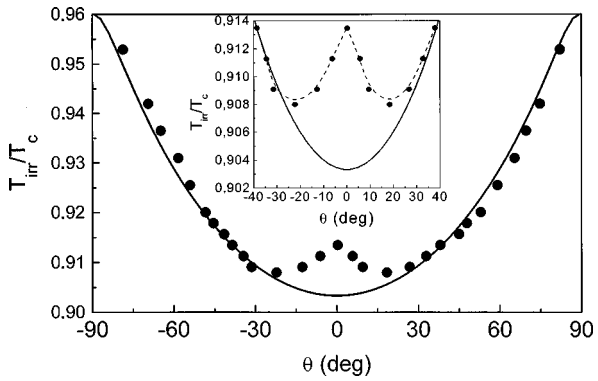

FIG. 6. Angular dependence of the irreversibility line for $H\|c$ for $H=3$ T. The continuous line shows the fitting of Eq. (3) to the anisotropic Ginzburg-Landau model. Also shown in the inset is a zoom of the central part, where the shift associated to the ''quenched'' Bose glass transition is clearly appreciated.

for 6 and 9 T collapse into a single curve as was shown in Fig. 3 for $t=T/T_c=0.995$. However data at 3 T diverge from this scaling for $H\varepsilon(\theta)>2.2$ T, which corresponds to $|\theta|<45°=|\theta_{\rm div}|$, indicating that we cannot collapse all curves into an universal curve at this temperature. In the inset of Fig. 5, it is shown the corresponding magnetoresistance curve for $H=3$ T at $t\sim 0.931$. Note that the accommodation angle $\theta_{\rm acc}$ determined from this curve is $\theta_{\rm acc}\sim 15°$, which is much smaller than the angle $|\theta_{\rm div}|\sim 45°$ determined from the Eq. (2) scaling. This indicates that the region of discrepancy for the anisotropic Ginzburg-Landau model is larger than just the strict phase diagram region for which vortices are considered trapped in the twin boundaries as defined by $\theta_{\rm acc}$. This further confirms that the determination of the intrinsic anisotropy by this method based on angular magnetoresistance measurements must be performed at temperatures very near the mean-field $H_{c2}(T)$ transition. This same analysis performed at $t\sim 0.988$, where no sign of dissipation decrease was observed at $\theta\sim 0°$ from the magnetoresistance curves, already showed nonuniversal scaling law.

However, we have been able to determine the anisotropy of this material at low temperatures, from the angular dependence of the irreversibility line. Figure 6 shows the irreversibility line (IL) as a function of the angle θ for a magnetic field of 3 T as representative data. A criteria of $\rho/\rho_N=0.001$, ρ_N being the normal-state resistivity, has been used to determine the IL from the angular-dependent magnetoresistance measurements. A sudden upward shift of the IL for $|\theta|<30°$ is superimposed to a parabolic background. The continuous line of Fig. 6 is a fit to the anisotropic Ginzburg-Landau model expression of the irreversibility line. Assuming the validity of the scaling approach[36,39] this leads to

$$\varepsilon(\theta)H_{\rm irr}=H_0\left(1-\frac{T_{\rm irr}}{T_c}\right)^{\alpha}, \tag{3}$$

where $\varepsilon(\theta)$ is given by Eq. (2). Note that this model is able to fit the experimental data for all angles except for $|\theta|<30°$, the region where the irreversibility line is dominated by twin boundary pinning and therefore does not follow the effective-mass model. The values obtained for the fitting parameters of Eq. (3) are $H_0\sim 159$ T, $\alpha\sim 2.2$, and $\gamma^{-1}\sim 7$,

which are in good agreement with results reported for the Y123 system.[9] The experimental values for $|\theta|<30°$ have not been included in the fitting procedure since they have been ascribed to linearly correlated twin boundary pinning. This twin boundary pinning region on the angular-dependent irreversibility line is comparable to that observed for columnar tracks in U irradiated Y123 crystals and somewhat larger than the angular region observed for twinned single crystals.[9] This could be explained by the intrinsic mosaicity of melt-textured composites.[32] In particular, the value $\gamma^{-1}\sim 7$ obtained from the IL fitting is in perfect agreement with that obtained at $t=0.995$ from the angular-dependent magnetoresistance. This suggests that the intrinsic anisotropy is responsible for the parabolic function of the angular-dependent irreversibility line and that any isotropical microstructural pinning defect that might be active at these temperatures, like point defects or the ''quenched'' disorder induced by 211 particles, do not change the anisotropy of the material and may just shift slightly upwards the irreversibility line following Eq. (3).[36] This further confirms that the 211 particles in the liquid vortex state might be considered as isotropical random disorder. Consequently, we can also conclude that the anisotropic Ginzburg-Landau model is also valid at low temperatures to determine the intrinsic anisotropy of Y123/211 melt-textured composites if angles close to the c axis are avoided. And finally, that angular-dependent irreversibility line measurements, $T_{\rm irr}(\theta)$, allows us to determine the contribution of twin boundaries to the irreversibility line. In particular, we note that the irreversibility temperature shift in the present melt-textured composite, $\Delta T_{\rm irr}=T_{\rm irr}^{\rm TB}-T_{\rm irr}^{m}\sim 0.9$ K at 3 T and $\Delta T_{\rm irr}\sim 1$ K at 6 T is very similar to that observed in single crystals,[9,15] where $T_{\rm irr}^{\rm TB}$ is the maximum temperature of the irreversibility line observed at $H\|c$ and $T_{\rm irr}^{m}$ that corresponds to the anisotropic Ginzburg-Landau model fitting. This might indicate that the fundamental postulates of the Bose glass theory[13] for the irreversibility line transition detected in twinned single crystals might also be valid in Y123/211 composites in spite of the additional disorder introduced by 211 precipitates.

C. Vortex liquid phase diagram

Upon identification of the intrinsic anisotropy of the irreversibility line and the shift arising from twin boundaries, we are in a position to define the different regimes in the H-T phase diagram within the liquid vortex state.

Figure 7 shows the different H-T lines of the phase diagram separating the Bose glass solid (BGS) phase, partially entangled liquid or disentangled liquid phases (PEL or DL) and the entangled liquid phase (EL), for this particular Y123/211 melt-textured sample for $H\|c$ (closed symbols). The irreversibility line determined from the effective-mass model fitting (see Fig. 6) is indicated by $H_{\rm irr}^{m}(T)=100(1-T_{\rm irr}^{m}/T_c)^{1.5}$. This is the irreversibility line that would be observed in this melt-textured Y123/211 composite in the absence of twin planes. The presence of twin boundaries, however, leads to a new ''irreversibility line,'' $H_{\rm irr}^{\rm TB}=111(1-T_{\rm irr}^{\rm TB}/T_c)^{1.5}$, defined by the maximum of $T_{\rm irr}(\theta)$ (see Fig. 6). Note that at 77 K, the upward shift of $H_{\rm irr}^{\rm TB}$ arising from the vortex liquid state twin boundary pinning is ~ 1 T, which evidences once more that twin boundaries have a non-

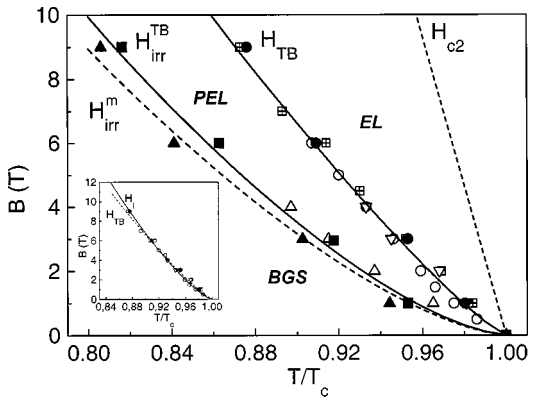

FIG. 7. Magnetic phase diagram of the liquid vortex state of Y123/211 melt-textured composites for $H\|c$. Indicated are: (▲) the intrinsic irreversibility line, $H_{\rm irr}^{m}(T)$, obtained from the anisotropic Ginzburg-Landau model, (■) the quenched Bose glass transition line due to twin boundary pinning, $H_{\rm irr}^{\rm TB}(T)$, and (●) the $H_{\rm TB}(T)$ transition indicating the transition from a partially entangled liquid to a fully entangled liquid. Also shown are the Bose glass transition for (△) a twinned single crystal, the $H_{\rm TB}(T)$ line for (⭘) a twinned Y123 single crystal and the $H^{*}(T)$ line for (⊞) a Y123/211 melt-textured composite and (▽) a twinned single crystal both obtained from flux transformer experiments. The mean field $H_{c2}(T)$ and the regions indicating the Bose glass solid (BGS), partially entangled liquid (PEL), or disentangled liquid (DL) for the case of single crystals and, the entangled liquid (EL) phases, are also represented. In the inset, all four $H_{\rm TB}(T)$ data sets are again shown and compared to the fit to the scaling law $H_1/|t|^{2\nu}=$const with $\nu=0.699$ suggested by Nguyen and Sudbo (Ref. 21) and the best fit $H_{\rm TB}(T)=105(1-T_{\rm TB}/T_c)^{1.2}$ shown in their Fig. 7.

negligible effectiveness as pinning center in melt-textured composites at least for $H\|c$. Similar conclusions were achieved from magnetization measurements in the solid vortex phase of J_c^{c} (Ref. 35) and from transport current measurements for $H\|ab$ when the pinning force remains parallel to the ab plane.[40] Also shown in Fig. 7 is the Bose glass transition for a twinned single crystal (open symbols).[41] Notice that both transitions, the irreversibility line for the melt-textured composite $H_{\rm irr}^{\rm TB}$ and the Bose glass transition for the twinned single crystal, do have similar behaviors, suggesting the Bose glass character of the $H_{\rm irr}^{\rm TB}(T)$ line also for melt-textured composites. Additional experimental analysis to identify the character of this transition is required and a comparison with the extensive scaling analysis of the transport properties performed in twinned single crystals,[15] from where the second-order character of the Bose glass transition was identified, is necessary.

Additionally, Fig. 7 indicates the $H_{\rm TB}(T)$ line defined for each magnetic field as that temperature below which the magnetoresistance curve evidences a dip for $\theta\sim 0°$ (see Fig. 4). This new $H_{\rm TB}$ line corresponds to the onset of twin boundary pinning and hence determines the region of the phase diagram below which twin boundary pinning starts to enhance tilt rigidity of the vortices and vortex localization at the twin boundaries. The phase diagram region between $H_{\rm irr}^{\rm TB}$ and $H_{\rm TB}$ defines the partially entangled or disentangled liquid vortex phase characterized by a vortex liquid state dominated by the linearly correlated twin boundary pinning and hence, with a modified resistivity according to the change in

the liquid viscosity introduced by this correlated defect.[36] Indicated in Fig. 7, are the H_{TB} lines for our Y123/28 wt. % 211 melt-textured composite (closed symbols) compared with the H_{TB} line equally determined by Fleshler *et al.*[10] for a twinned Y123 single crystal, and the so-called $H^*(T)$ line previously defined by López *et al.*[41] and Galante *et al.*[20] from a flux transformer experiment for twinned single crystal and a melt-textured Y123/28 wt. % 211, respectively. Notice the unique transition defining the $H_{TB}(T)$ line for both melt-textured and twinned single crystals, which once more denotes the high-crystalline quality of Y123/211 composites and suggests the intrinsic character of $H_{TB}(T)$ for densely twinned samples. Contrary to clean crystals, where the solid-to-liquid vortex state is mediated by the melting transition $H_m(T)$ in densely twinned crystals it has been demonstrated[17] that the solid Bose glass state is transformed into a disentangled liquid at $H_{irr}(T)=H_{BG}(T)$ and this to an entangled liquid at $H_{TB}(T)$. Twin boundaries then act as correlated defects promoting disentanglement, and taking into account that $H_{BG}(T)$ lies above $H_m(T)$,[10,42] twin boundaries are seen to stabilize the solid phase of vortex lines.

Flux transformer experiments in single crystals,[41] have detected an anisotropic zero resistance behavior below a $H^*(T)$ transition, which coincides with the $H_{TB}(T)$ line (see Fig. 7). This region of the liquid phase diagram is characterized by a full *c*-axis correlation of the vortex threading the whole crystal, thus corroborating the condition of a disentangled vortex liquid phase.[36] However, flux transformer studies on the $H^*(T)$ dependence with the crystal thickness[16] have shown that the full *c*-axis coherence is lost for thick crystals. The same experiments performed on bulk 123/211 composites[20] have identified an $H^*(T)$ line at the H-T point of the phase diagram above which vortex velocity in the top and bottom sides of the sample become completely uncorrelated. Below this $H^*(T)$ line, it was found that $V_{top}=fV_{bottom}$, f being a weakly dependent factor ($f\sim 1.34$ in those particular samples) and zero-resistance state was achieved at the same temperature both when $I\|c$ and $I\|ab$. This liquid vortex phase was defined as partially entangled in the sense that vortex correlation along the *c* axis was short ranged. Figure 7 also shows this $H^*(T)$ transition for melt-textured composites.

Remarkably, all four experimental data sets drawn in Fig. 7 and identified as $H_{TB}(T)$ or $H^*(T)$ have been described by the same fitting curve independently from the measuring technique and type of sample considered, i.e., single-crystal or melt-textured composite, namely,

$$H_{TB}=H_0^{TB}\left(1-\frac{T_{TB}}{T_c}\right)^n, \tag{4}$$

with $H_0^{TB}\sim 105$ T and $n\sim 1.2$, thus pointing out a unique physical origin for all these lines and for the DL and PEL vortex phases.

Galante *et al.*[20] proposed that the presence of the randomly distributed 211 particles in the 123 matrix of melt-textured composites could be the cause of the correlation length reduction observed in the PEL phase (i.e., $H_{irr}<H<H^*=H_{TB}$). These 211 precipitates manifest as ''quenched'' disorder against the stabilization of a long-range correlated vortex liquid by promoting local vortex deformation.[43] Thus, twin boundaries pin shorter segments of vortices and flux cutting and recombination processes are expected to be enhanced. The $H_{irr}^{TB}(T)$ transition would then reflect a ''quenched'' Bose-like glass transition[36] where the correlation of vortices along the *c* axis is only finite and so no true second-order phase transition might be achieved. Still both transitions, the true Bose glass transition for a twinned single crystal[41] and the ''quenched'' Bose-like glass transition $H_{irr}^{TB}(T)$ for our melt-textured composite, do have similar behaviors as shown in Fig. 7 for these two particular samples.

Further support on the fact that in melt-textured composites ''quenched'' disorder is relevant to promote flux cutting and recombination processes by perturbing, though not overwhelming, the effect of correlated disorder, is found in results of the magnetic field dependence of the pinning energy obtained from thermally activated Arrhenius plots. A $U\propto H^{-0.5}$ dependence for $H\|c$, theoretically ascribed to plastic flow and flux-cutting processes[23,44,45] and experimentally observed in quenched disordered Bi-2212–based thin films,[46] is found for melt-textured material.[38] The expected $U\propto H^{-1}$ law, experimentally found for linearly correlated pinning centers like columnar tracks in single crystals,[37] has not been obtained in melt-textured composites.

Additionally, the fact that the four lines shown in Fig. 7 corresponding to single-crystals and Y123/211 composites superpose, evidences that the two experimental ways [$H^*(T)$ and $H_{TB}(T)$] of determining the transition to an entangled liquid are valid and, that this transition does not depend on the *c*-axis vortex correlation length but, on the competition between the twin boundary pinning energy per unit length and the thermal energy.

We would also like to note that Nguyen and Sudbo[21] have claimed from large-scale Monte Carlo simulations of vortex lattice systems without disorder, that an intrinsic phase transition may occur within the liquid vortex phase characterized by a loss of vortex line tension. This would be an intrinsic phase transition of high-T_c superconductors, which should be independent of the specific material and microstructural defects, though probably only through the material defects would it be possible to experimentally detect it. This new $H_1(T)$ line should be consistent with the scaling law $H/|t|^{2\nu}=$const, where $\nu=0.669$ and $t=(T_c-T_L)/T_c$, which is characteristic of the 3D anisotropic *XY* Hamiltonian modeling for extreme type-II superconductors. Although the results shown in the inset of Fig. 7 quite agree with this theory [see the $H_{TB}(T)$ line in comparison with this $H_1(T)$ line], further analysis at higher fields are required for the present sample and other high-T_c materials being dominated by other defects, to disregard any possible coincidence with a crossover depinning line.

Finally, in Fig. 8 we show the first experimental determination of a complete angular-dependent magnetic phase diagram of a melt-textured composite. Results for a magnetic field of 3 T are presented as representative data. Indicated are the Bose glass and vortex glass (VG) solid phases and the partially entangled and entangled liquid phases determined form the angular-dependent magnetoresistance measurements presented above. The angular dependence of IL has allowed us to separate (see Fig. 6) the background contribu-

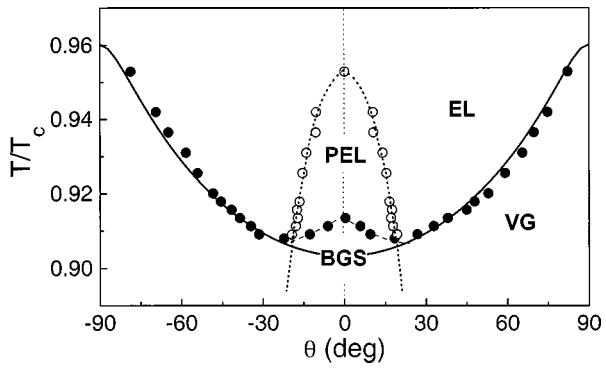

FIG. 8. Angular dependence of the magnetic phase diagram at $H=3$ T. Indicated are (●) the angular dependence of the irreversibility line together with the fit to the anisotropic Ginzburg-Landau model (continuous line), and (⊙) the angular dependence of the accommodation angle θ_{acc}. The dotted line is a guide for the eye. These results have allowed us to define the different regions of the phase diagram: Bose glass solid (BGS) phase, Vortex glass (VG) solid phase, partially entangled liquid (PEL) vortex phase, and entangled liquid (EL) vortex phase for the melt-textured Y123/211 composite.

tion ascribed to quenched disorder and intrinsic material anisotropy from the cusplike irreversibility line near $\theta\sim 0$ induced by the linearly correlated twin boundary defects. This enables us to distinguish a VG solid phase and a BGS phase, respectively. Also shown are the experimental results for the angular-dependent $H_{TB}(T)$ transition at $H=3$ T (open symbols) identified from the temperature dependence of the accommodation angle (see Fig. 4). The region between $T_{TB}(\theta)$ and $T_{irr}^{TB}(\theta)$ is thus associated to the PEL phase. Hence, two different transitions can be found to enter into the entangled liquid state, either through the PEL or directly from the VG at angles larger than those affected by the linearly correlated twin boundary disorder. Quenched disorder from the 211 particles is proposed as the main disorder to undergo the VG transition while linearly correlated twin boundary disorder promotes the PEL transition. A triple point joining the BGS, VG solid, and PEL phases can then be identified. We note that beyond this triple point, in sparsely twinned single crystals,[47] the first-order melting transition has been recovered when crossing to the solid phase from the EL phase.

IV. CONCLUSIONS

Angular-dependent magnetoresistance measurements, $\rho(T,H,\theta)$, of $YBa_2Cu_3O_7/Y_2BaCuO_5$ melt-textured composites have been used to determine the intrinsic anisotropy of the superconducting state of this material. The anisotropic Ginzburg-Landau model has been identified as valid for describing the anisotropy of the field and angular-dependent resistivity of $YBa_2Cu_3O_7/Y_2BaCuO_5$ melt-textured composites, at temperatures very near T_c where flux-pinning effects have been washed out by thermal activation. Anisotropy values typical of single crystals, i.e., $\gamma^{-1}\sim 7$, have been obtained.

The same measurements at lower temperatures, have been used to define the H-T-θ magnetic phase diagram of Y123/211 melt-textured composites. The BGS, VG solid, PEL, and EL phases have been determined. Twin boundaries have been proven to be efficient as linearly correlated pinning centers in the PEL phase in melt-textured composites. The transition from the PEL to the EL phase $[H_{TB}(T)]$ has been compared to that of a Y123 twinned single crystals and we have experimentally concluded that in spite of the complex microstructure of Y123/211 composites, the same laws seem to determine these two transitions to the EL state. The randomly distributed 211 particles are seen to be relevant to induce shorter c-axis vortex correlation lengths by promoting flux cutting in the PEL phase though correlated disorder by twin boundaries is determined as the prominent disorder. The quenched disorder induced by the 211 particles is proposed as the main disorder inducing the transition from the EL to the VG in melt-textured composites.

ACKNOWLEDGMENTS

Financial support from CICYT (Nos. MAT96-1052 and MAT96-904), Generalitat de Catalunya (No. 1997 SGR 26), and Supercurrents (EU-TMR Network No. ERBFMRXCT98-01289) is acknowledged. T.P. wishes to thank Ministerio de Educación y Cultura (Programa Incorporación de Doctores) for financial support.

[1] H. Safar, P. L. Gammel, D. A. Huse, D. J. Bishop, J. P. Price, and D. M. Ginzberg, Phys. Rev. Lett. **69**, 824 (1992).
[2] W. K. Kwok, S. Fleshler, U. Welp, V. M. Vinokur, S. Downey, and G. W. Crabtree, Phys. Rev. Lett. **69**, 3370 (1992).
[3] U. Welp, J. A. Fendrich, W. K. Kwok, G. W. Crabtree, and W. B. Veal, Phys. Rev. Lett. **76**, 4809 (1996).
[4] A. Schilling, R. A. Fisher, N. E. Phillips, U. Welp, D. Dasgupta, K. W. Kwok, and G. W. Crabtree, Nature (London) **382**, 791 (1996).
[5] L. Civale, A. D. Marwick, M. W. Elfresh, T. K. Worthington, A. P. Malozermoff, F. H. Holtzberg, J. R. Thompson, and M. A. Kirk, Phys. Rev. Lett. **65**, 1164 (1990).
[6] L. M. Paulius, R. E. Shamu, S. Ferguson, M. C. de Andrade, and M. B. Maple, Appl. Phys. Lett. **71**, 3415 (1997).
[7] L. Civale, A. D. Marwick, T. K. Worthington, M. A. Kirk, J. R. Thompson, L. Krusin-Elbaum, Y. Sun, J. R. Clem, and F. Holtzberg, Phys. Rev. Lett. **67**, 648 (1991).
[8] M. Konczykowski, F. Rullier-Albenque, R. E. Yacoby, A. Shaulov, Y. Yeshurum, and P. Lejay, Phys. Rev. B **44**, 7167 (1991).
[9] L. M. Paulius, J. A. Fendrich, W. K. Kwok, A. E. Koshelev, V. M. Vinokur, G. W. Crabtree, and B. G. Glagola, Phys. Rev. B **56**, 913 (1997).
[10] S. Fleshler, W. K. Kowk, U. Welp, V. M. Vinokur, M. K. Smithm, J. Downey, and G. W. Crabtree, Phys. Rev. B **47**, 14 448 (1993).
[11] V. K. Vlasko-Vlasov, L. A. Dorosinski, A. A. Polyanskii, V. I. Nikitenko, U. Welp, B. W. Veal, and G. W. Crabtree, Phys. Rev. Lett. **72**, 3246 (1994).
[12] D. S. Fisher, M. P. A. Fisher, and D. A. Huse, Phys. Rev. B **43**, 130 (1991).
[13] D. R. Nelson and V. M. Vinokur, Phys. Rev. B **48**, 13 060 (1993).
[14] W. K. Kwok, U. Welp, G. W. Crabtree, K. G. Vandervoort, R.

Hulscher, and J. Z. Liu, Phys. Rev. Lett. **64**, 966 (1990).
[15] S. A. Griega, E. Morré, E. Osquiguil, C. Balseiro, G. Nieva, and F. de la Cruz, Phys. Rev. Lett. **81**, 2348 (1998).
[16] D. López, E. F. Righi, G. Nieva, F. de la Cruz, W. K. Kwok, J. A. Fendrich, G. W. Crabtree, and L. Paulius, Phys. Rev. B **53**, 8895 (1996).
[17] H. Safar, P. L. Gammel, D. A. Huse, S. N. Majumdar, L. F. Schneemeyer, D. J. Bishop, D. López, G. Nieva, and F. de la Cruz, Phys. Rev. Lett. **72**, 1272 (1994).
[18] M. Murakami, in *Proceedings and Properties of High T_c Superconductors*, edited by S. Jin (World Scientific, Singapore, 1993), Vol. 1, Chap. 6, pp. 215–268.
[19] B. Martínez, X. Obradors, A. Gou, V. Gomis, S. Piñol, J. Fontcuberta, and H. Van Tool, Phys. Rev. B **53**, 2797 (1996).
[20] F. Galante, E. Rodriguez, J. Fontcuberta, and X. Obradors, Physica C **296**, 96 (1998).
[21] A. K. Nguyen and A. Sudbo, Europhys. Lett. **46**, 780 (1999).
[22] N. Vilalta, F. Sandiumenge, S. Piñol, and X. Obradors, J. Mater. Res. **12**, 38 (1997).
[23] J. A. Fendrich, W. K. Kwok, J. Giapintzakis, C. J. can der Beek, V. M. Vinokur, S. Fleshler, U. Welp, H. K. Viswamathan, and G. W. Crabtree, Phys. Rev. Lett. **74**, 1210 (1995).
[24] M. Tinkham, Physica C **235**, 3 (1994).
[25] M. S. Osofsky, R. J. Soulen, S. A. Wolf, J. M. Broto, H. Rakoto, J. C. Ousset, G. Coffe, S. Askenazy, P. Pari, I. Bozovic, J. N. Eckstein, and G. F. Virshup, Phys. Rev. Lett. **71**, 2315 (1991).
[26] G. Blatter, V. B. Geshkenbein, and A. I. Larkin, Phys. Rev. Lett. **68**, 875 (1992).
[27] M. J. Naughton, R. C. Yu, P. K. Davies, J. E. Fischer, R. V. Chamberlin, Z. Z. Wang, T. W. Jing, N. P. Ong, and P. M. Chaikin, Phys. Rev. B **38**, 9280 (1988).
[28] U. Welp, K. W. Kwok, G. W. Crabtree, K. G. Vandervoort, and J. Z. Liu, Phys. Rev. Lett. **62**, 1908 (1989).
[29] D. E. Farrell, C. M. Williams, S. A. Wolf, N. P. Bansal, and V. G. Kogan, Phys. Rev. Lett. **61**, 2805 (1988).
[30] M. Vélez, E. M. González, J. I. Martín, and J. L. Vicent, Phys. Rev. B **54**, 101 (1996).
[31] W. K. Kwok, J. Fendrich, S. Fleshler, U. Welp, J. Downey, G. W. Crabtree, and J. Giapintzakis, Physica B **197**, 579 (1994).
[32] F. Sandiumenge, B. Martínez, and X. Obradors, Supercond. Sci. Technol. **10**, A93 (1997).
[33] K. Schönman, B. Secbacker, and K. Andres, Physica C **184**, 41 (1991).
[34] L. S. Uspenskaye, V. K. Vlasko-Vlasov, V. I. Nikitenko, and T. H. Johansen, Phys. Rev. B **56**, 11 979 (1997).
[35] B. Martínez, T. Puig, A. Gou, V. Gomis, S. Piñol, J. Fontcuberta, X. Obradors, and G. Chouteau, Phys. Rev. B **58**, 15 198 (1998).
[36] G. Blatter, V. M. Feigel'man, V. S. Geshkenbein, A. I. Larkin, and V. M. Vinokur, Rev. Mod. Phys. **66**, 1125 (1994).
[37] W. Kwok, L. Paulius, V. M. Vinokur, A. M. Petrean, R. M. Ronningen, and G. W. Crabtree, Phys. Rev. Lett. **80**, 600 (1998).
[38] T. Puig and X. Obradors (unpublished).
[39] X. Xiaojun, F. Lan, W. Liangbin, Z. Yuheng, F. Jun, C. Xiaowen, L. Kebin, and S. Hisashi, Phys. Rev. B **59**, 608 (1999).
[40] S. Sanfilippo, A. Sulpice, O. Laborde, D. Bourgault, Th. Fournier, and R. Tournier, Phys. Rev. B **58**, 15 189 (1998).
[41] D. López, L. Krusin-Elbaum, H. Safar, E. Righi, F. de la Cruz, S. Griega, C. Field, W. K. Kwok, L. Paulius, and G. W. Crabtree, Phys. Rev. Lett. **80**, 1070 (1998).
[42] W. K. Kwok, J. A. Fendrich, C. J. van der Beek, and G. W. Crabtree, Phys. Rev. Lett. **73**, 2614 (1994).
[43] T. Hwa, D. R. Nelson, and V. M. Vinokur, Phys. Rev. B **48**, 1167 (1993).
[44] V. B. Geshkenbein, M. V. Feigel'man, A. I. Larkin, and V. M. Vinokur, Physica C **162-164**, 239 (1989).
[45] V. M. Vinokur, M. V. Feigel'man, V. B. Geshkenbein, and A. I. Larkin, Phys. Rev. Lett. **65**, 259 (1990).
[46] L. Miu, G. Jacob, P. Haiback, F. Hilmer, H. Adrian, and C. C. Almasan, Phys. Rev. B **57**, 3151 (1998).
[47] G. W. Crabtree, W. K. Kwok, U. Welp, D. López, and J. A. Fendrich, in *Proceedings of the NATO Advanced Study Institute on Physics and Material Science of Vortex States, Flux Pinning and Dynamics, Kusadosi, Turkey, 1998*, edited by R. Kossowsky, S. Bose, V. Pan, and Z. Durusoy (Kluwer, Dordrecht, 1999).